Published in final edited form as:
Nat Chem Biol. 2018 April ; 14(4): 396–404. doi:10.1038/s41589-018-0015-6.

An optically controlled probe identifies lipid-gating fenestrations within the TRPC3 channel

Michaela Lichtenegger[#1], **Oleksandra Tiapko**[#1], **Barbora Svobodova**[1], **Thomas Stockner**[2], **Toma N. Glasnov**[3], **Wolfgang Schreibmayer**[1], **Dieter Platzer**[1], **Gema Guedes de la Cruz**[3], **Sarah Krenn**[1], **Romana Schober**[4], **Niroj Shrestha**[1], **Rainer Schindl**[1], **Christoph Romanin**[4], and **Klaus Groschner**[1,*]

[1]Gottfried Schatz Research Center, Biophysics, Medical University of Graz, Graz, Austria

[2]Institute of Pharmacology, Medical University of Vienna, Vienna, Austria

[3]Institute of Chemistry, University of Graz, Graz, Austria

[4]Institute of Biophysics, University of Linz, Linz, Austria

[#] These authors contributed equally to this work.

Abstract

Transient receptor potential canonical (TRPC) channels TRPC3, TRPC6 and TRPC7 are able to sense the lipid messenger diacylglycerol (DAG). The DAG-sensing and lipid-gating processes in these ion channels are still unknown. To gain insights into the lipid-sensing principle, we generated a DAG photoswitch, OptoDArG, that enabled efficient control of TRPC3 by light. A structure-guided mutagenesis screen of the TRPC3 pore domain unveiled a single glycine residue behind the selectivity filter (G652) that is exposed to lipid through a subunit-joining fenestration. Exchange of G652 with larger residues altered the ability of TRPC3 to discriminate between different DAG molecules. Light-controlled activation–deactivation cycling of TRPC3 channels by an OptoDArG-mediated optical ‘lipid clamp’ identified pore domain fenestrations as pivotal elements of the channel´s lipid-sensing machinery. We provide evidence for a novel concept of lipid sensing by TRPC channels based on a lateral fenestration in the pore domain that accommodates lipid mediators to control gating.

The canonical subfamily of TRPCs includes transmembrane proteins that have the unique ability to recognize the lipid mediator DAG1 and to translate this chemical information into cation permeation as well as changes in membrane potential. These nonselective cation channels are tightly linked to essential phospholipase C (PLC)-coupled signaling pathways and control Ca^{2+}-dependent effector systems in a coordinated manner in a wide range of mammalian tissues. DAG-gated TRPC conductances contribute both to physiological control of tissue and organ function2–6 and to maladaptive remodeling processes and pathologies7–

[*] klaus.groschner@medunigraz.at.

Author contributions

M.L. and O.T. performed experiments, analyzed data and wrote parts of the manuscript; T.S. performed homology modeling; B.S., D.P., W.S., R. Schober, N.S., S.K. and R. Schindl analyzed data; T.N.G. and G.G.d.l.C. synthesized compounds; C.R. contributed with experimental planning and data interpretation; K.G. designed the project and wrote the manuscript.

Europe PMC Funders Author Manuscripts

11. However, a comprehensive molecular concept of lipid signaling via DAG-sensitive TRPC3, TRPC6 and TRPC7 channels and a mechanistic understanding of the lipid-sensing machinery is still lacking. In general, researchers have considered both direct and indirect lipid-sensing hypotheses; namely, direct molecular recognition of lipids by the channel protein or indirect transfer of molecular information such as lipid-mediated changes in membrane architecture or lateral tension detected by a process of mechanosensation12. Studies have provided evidence for regulation of TRP channels by lipids and hydrophobic ligands via direct lipid–protein interactions either at the cytosolic elements in the channels13,14 or by binding into hydrophobic crevices and clefts within the pore-forming domain, including areas near the selectivity filter15,16. Attempts to gather information about this fundamental and pathophysiologically important biological principle have been hampered by the difficulties inherent to accurately determining and controlling the quantity of lipid mediators in cell membranes. To demonstrate that mutations have altered the discriminative power of channels and the potency of lipid mediators, it is necessary to quantitatively or at least semiquantitatively characterize the effects of lipids on the TRPC conductance. The recent advent of photochromic lipid mediators, which allow precise temporal and quantitative control of the bioactive lipid species within membranes17,18, has generated a considerable advance in lipid pharmacology. Several azobenzenecontaining photochromic DAGs have recently been produced18. The biological activity of these compounds is efficiently controlled by light, as they harbor azobenzene moieties within aliphatic side chains, and their biological activity is governed by light-dependent cis–trans isomerization. Consequently, we generated photoswitchable DAGs, characterized these tools at the electrophysiological level and identified a novel photochromic DAG featuring two arachidonyl-mimetic photoswitchable azobenzene chains, termed OptoDArG, as a highly efficient photocromic ligand for the control of TRPC3 activity. We employed this tool together with a structureguided mutagenesis approach to test for lipid recognition within the pore domain of TRPC3. Our findings show that a novel DAG photoswitch (OptoDArG) can be successfully applied for mechanistic analysis of lipid signaling in ion channels and identify a hydrophobic fenestration that constitutes a subunit interface behind the TRPC3 selectivity filter and harbors residues critical for DAG recognition and channel gating.

Results

A novel DAG photoswitch for efficient control of TRPC3. The recent introduction of light-controlled lipid structures represented a substantial technological advance that enabled researchers to temporally control the active quantity of lipid mediators in membranes with a high degree of accuracy. To employ this strategy for the examination of lipid-gating processes in TRPC channels, we first synthetized PhoDAG-1 (**1**), a recently introduced photoswitchable analog of 2-O-arachidonyl-1-O-stearoyl-sn-glycerol (1,2-SAG)18 and tested its suitability for the control of TRPC3 channels by light. As illustrated in Fig. 1a, PhoDAG-1 (400 μ M) indeed allowed us to temporally control the TRPC3 conductance. To initiate photoconversion to cis-PhoDAG-1 upon illumination with ultraviolet (UV) light, we evoked a conductance with TRPC3 characteristics in HEK293 cells expressing TRPC3, but not in nontransfected controls (Supplementary Fig. 1). However, TRPC3 current densities were minute and were clearly lower than those typically obtained by stimulation of the

endogenous PLC pathway. The biological activity of DAGs appears to be dependent on the degree of saturation1, and we therefore synthetized and tested a modified DAG containing two moieties of the arachidonic acid mimetic azobenzene side chain, which was designated as OptoDArG (2; Supplementary Note and Fig. 1b). OptoDArG, like PhoDAG-1 (ref. 18), adopts the trans conformation in the dark, is rapidly converted into the cis conformation by UV light (340 nm) and can be reverted to the trans conformation by illumination with blue light (430 nm). In its trans form, OptoDArG (30 μM) had no significant effect on basal conductances in TRPC3-expressing cells and did not affect membrane conductances of nontransfected HEK293 cells (Supplementary Figure 1); photoisomerization to the cis conformation rapidly and reversibly activated the expressed TRPC3 conductance to levels that were comparable to its activation via PLC stimulation and thus were significantly higher than that achieved with PhoDAG-1 (Figure 1c; for a comparison, see Figure 3a).

Photoactivation of OptoDArG did not change membrane conductances of nontransfected HEK cells (Supplementary Fig. 1). As recently reported for PhoDAG-1 (ref. 18), OptoDArg rapidly initiated translocation of PKCα from the cytosol to the plasma membrane (Supplementary Fig. 2). The maximum levels of TRPC3 activation were reached after about 30 s (2–3 cycles of repetitive activation), and a rapid inactivation phase was observed, mimicking the behavior of native TRPC3 conductanes19. Peak current levels were rapidly restored during repetitive cycling between active and inactive lipid conformations. This demonstrates that a second, relatively slow process of channel activation–potentiation is taking place, and this process and TRPC3 inactivation are preserved when the channel is controlled by the lipid photoswitch.

The cis-OptoDArG-induced conductance displayed the characteristic double-rectifying feature of TRPC3 conductances (Figure 1d). For the first time, the results of these experiments allowed us to demonstrate effective optical control of TRPC3 channels at the ionic conductance level (Figure 1c,d). Once we had OptoDArG as a potent photopharmacological tool in hand, we set out to test for the role of residues in the TRPC3 pore domain in DAG recognition, taking an approach that was comprised of structure-guided mutagenesis and lipid photopharmacology.

G652 is a critical determinant of lipid gating in TRPC3. Gating of TRP channels by lipid activators potentially involves movement in the outer pore region, including structures adjacent to the selectivity filter, as exemplified for TRPV1 (ref. 15). Consequently, we screened for residues within the TRPC3 pore domain that had the potential to determine DAG sensitivity. Figure 2a shows a sequence alignment of the pore regions of TRPC proteins encompassing the pore helix, pore loop and the adjacent stretch of the S6 helix. This highly conserved part of the channels harbors residues that have been previously identified as critical for channel function, such as the LFW motif, mutations of which have been found to retain the membrane-targeting ability of TRPC channels but disrupt their function in a dominant negative manner20. The fact that mutations in the LFW sequence result in complete lack of agonist- or lipid-induced permeation precluded a more detailed investigation as to whether the permeation pathway or the lipid-gating process is affected. We have previously identified hydrophilic residues lining the permeation pathway of TRPC3, including the key negatively charged residue (E630) in the selectivity filter by

homology modeling6,21. This homology model was used as the basis of a structure-guided mutagenesis strategy to further identify conserved residues that are potentially exposed to membrane lipid and involved in lipid recognition and gating.

Our previously established homology model predicts the presence of lateral clefts (Figure 2b,c) that constitute subunit-joining fenestrations within the pore complex and expose residues behind the selectivity filter to the lipid bilayer (Figure 2c). Our goal was to investigate the role of these residues in lipid recognition and gating and to identify mutations that specifically alter TRPC3 lipid regulation while retaining basic channel functions. To do so, we characterized membrane targeting, constitutive activity and sensitivity to agonist–PLC activation and to a novel nonlipid activator (GSK1702934A19). By analyzing a series of mutations in this region (Supplementary Table 1), we identified residues whose mutation retained both correct membrane targeting and ion channel function (Supplementary Figure 3a). F618 represents a potential hydrophobic interaction site facing membrane lipids, and its exchange to alanine was found to generate channels that had basal activity comparable to wild-type channel complexes, whereas both agonist- or PLC-mediated activation and GSK1702934A-induced activation was eliminated (Supplementary Figure 3b,c). More interestingly, another residue, G652, was identified in which mutations (to A or L) displayed impaired basal and PLC stimulated channel functions. Nonetheless, sensitivity to activation by GSK1702934A was preserved. Both amino acids reside in a region that constitutes a subunit interface within S6 and parts of the selectivity filter and are situated within a lateral hydrophobic fenestration toward the lipid bilayer. G652 is positioned directly behind the selectivity filter (Figure 2) and is expected to provide flexibility for gating movements within the pore domain. Exchange of G652 for larger residues resulted in a size-dependent, graded reduction in PLC regulation, as shown for the responses of G652A and G652L mutations expressed in HEK293 cells (Figure 3a and Supplementary Table 1). Additional support for the critical role of G652 in lipid sensitivity is provided by the fact that mutation of G652A resulted in elimination of activation upon direct bath application of SAG (100 μM; Figure 3b), a highly effective agonist of lipid DAG-regulated TRPC channels1. Importantly, this residue is conserved throughout the TRPC family (Figure 2), and a mutation of the corresponding residue in TRPC6 (G709A) profoundly blunted PLC-mediated activation (Supplementary Figure 4).

To analyze effects of the G652A mutation on TRPC3 channel function in more detail, we performed single-channel recordings in HEK293 cells expressing either wild-type (WT) or mutant channels in the cell-attached patch configuration. The cells were exposed to muscarinic receptor stimulation by carbachol (CCh; 100 μ M; Figure 3c,d and Supplementary Figure 5a), and single channel activity was recorded when transient increases in N*Po (mean number of open channels) had declined to a stable, but still moderately enhanced, level of activity (after 2–5 min administration for TRPC3-WT and 5–20 s for G652A; Supplementary Figure 5b).

Channel activity was essentially low in patches of cells expressing the TRPC3-G652A mutant channels and displayed unchanged unitary conductance properties (Supplementary Figure 6), with a double-rectifying current–voltage (I–V) relation displaying moderate voltage dependence of both gating and permeability of TRPC3 channels. These results

indicated that both gating and permeability of TRPC3 channels were moderately voltage dependent, suggesting that gating is associated with rearrangements in the permeation pathway. Gating behavior in terms of open and closed dwell times were clearly altered in G652A channels. Therefore, we attempted to characterize the changes in the agonist- and PLC-induced gating behavior introduced by this pore-domain mutation. Single-channel recordings lacking overlapping openings and allowing interpretation of open dwell times as well as opening frequencies were selected. As illustrated in Figure 3c,d and Supplementary Figure 5a,b, the G652A channels exhibited remarkable differences in their gating behavior. Characteristic G652A open times were significantly longer than those of WT (Supplementary Figure 7). The results of our single-channel analysis demonstrated that activation of TRPC3 channels by the receptor–PLC pathway is not associated with a prolongation in the open times, but rather with an increase in opening frequency (Figure 3c), and hence appears based on the destabilization of closed states by the lipid mediator. This conclusion was also supported by evidence gathered in a few experiments that allowed us to inspect the closed dwell times and observe a single functional channel in the patches; namely, that the closed times were shortened (Figure 3c,d). In G652A mutant channels, CCh stimulation failed to increase opening frequency (Figure 3d). For most of the channels analyzed, closed-time distributions were best fitted by 3–4 exponentials, with G652A channels residing preferentially in long-lived closed states (Figure 3d). Our findings indicated that, at the single-channel level, the G652A mutation rendered the channel less sensitive to lipid-induced destabilization of closed states in the physiological setting of receptor–PLC stimulation. At this point, two distinct mechanistic concepts were considered: (i) G652 functions as a flexible linker in the gating machinery of the TRPC3 pore domain. Glycine residues provide conformational flexibility that no other amino acid can, and the introduction of a larger amino acid, creating rigidity, would suppress gating movements downstream of lipid recognition; (ii) alternatively, G652 serves not merely as a gating hinge but also is itself an integral part of the lipid recognition and sensing machinery, which is formed by fenestration, allowing certain lipids to penetrate into the pore domain. Importantly, G652A channels were found to be fully responsive to activation by the small-molecule activator GSK1702934A (Supplementary Table 1 and Supplementary Figure 3c), arguing against a general impairment of the channels´ gating machinery.

G652 serves recognition of DAGs by TRPC3

To address the role of G652 in the ability of TRPC3 to recognize DAG molecules, we next used conventional pharmacological tools to test whether the order of activation efficacy for a series of DAGs was altered in G652A. When challenging channels with different DAGs at 100 μM, we observed the efficacy order of OAG > SAG > DiC8 for the activation of TRPC3-WT channels (Figure 4a). In the G652A mutant, however, the activation preference was DiC8 > OAG > SAG (Figure 4b). OAG (2-O-acetyl-1-O-oleoyl-sn-glycerol) has been previously described as highly effective in terms of TRPC3 activation, considerably surpassing DiC8 (1,2-O-dioctanoyl-sn-glycerol, 1,2-DOG) as an agonist1. In striking contrast, G652A channels more readily accepted DiC8 over OAG as an activating species, whereas G652L displayed generally reduced lipid sensitivity. This result indicated that the G652A mutation not only resulted in a loss of function, but also, in fact, in a modification of the channel´s ability to recognize and discriminate among lipid mediators.

Interestingly, substituting glycine with alanine, which was expected to reduce gating flexibility, resulted in retrieval of function with respect to DiC8 activation (Figure 4). This finding does not provide support for the hypothesis that a general disruption of gating movements occurs downstream of primary lipid recognition in the protein. We hypothesized that G652 and proximate residues are crucial for molecular recognition of DAGs and hence may form part of a primary lipid-sensing structure. This concept was tested by using our newly developed photopharmacological tool. Reversible photoactivation by PhoDAG-1, which represents an active structural analog of SAG, was indeed eliminated in the G652A mutant (Figure 5a). These findings are consistent with those obtained using conventional SAG administration (Figures 3 and 4). In contrast, G652A channel activation by our new TRPC3-activating, photochromic ligand, OptoDArG, was facilitated (Figures 5b), as was activation by DiC8 (Figures 4). Of note, the corresponding G709A mutation in TRPC6 reduced sensitivity to photoactivation by OptoDArG (Supplementary Figure 8). These results supported the hypothesis that mutation of G652 alters the ability of the channel to sense DAGs and to discriminate their molecular structure. As noted above, the peak currents obtained during cyclic channel activation–deactivation instigated by OptoDArG at submaximum light intensities closely resembled the time course seen with the bath application of DAGs (Figure 3), which displayed an initial phase of time-dependent potentiation followed by inactivation and desensitization (Figures 1b and 5a). Moreover, repetitive activation–deactivation cycling in the TRPC3 G652A mutant at submaximum light intensities also resulted in increasingly incomplete deactivation, which was evident from elevations in the current levels that occurred during photoconversion to the inactive trans form, a phenomenon that was less prominent in TRPC3-WT channels (Figures 1). Incomplete deactivation of the G652A mutant channel upon deactivation by photoconversion to trans-OptoDArG was discernible only at higher light intensities, which were also associated with substantial inactivation or desensitization. Consequently, we first set out to define changes in lipid sensitivity from the mutation at low intensities to determine the threshold of activation. As the photopharmacological approach allowed us to exert precise spatiotemporal control over the relative levels of bioactive DAG quantities, we increased the active DAG level in a graded manner to delineate the threshold for activation by the lipid mediator. Thus, we established OptoDArG quantity–activity relations for WT and mutant channels by sequentially increasing the activating light intensities (Figure 5c).

The threshold for activation was shifted to lower light intensities in G652A mutant channels as compared to WT channels, with significant responses being observed at slightly lower light intensities (Figure 5d). Although potentiation and desensitization phenomena were barely evident at low light intensities, we cannot exclude an overlap of such slower gating processes with rapid photopharmacological activation–deactivation, especially at higher lipid-mediator levels. Therefore, our ability to precisely delineate maximum responses and potencies was hampered. Notably, we again observed a moderate elevation of current levels during deactivation at increasing light intensities, but only in the mutant. The fact that current levels during deactivation increased in an activation light-intensity-dependent manner (Figure 5d) may be explained either by enhanced potency of the lipid activator or by a slowed photoconversion of the photochromic lipid while it is associated with the channel complex. Moreover, a cooperative mechanism of lipid activation was considered that

requires lipid exchange at multiple hydrophobic recognition sites to trigger a concerted structural rearrangement and channel opening. The G652A mutation may alter cooperativity by changing either the number of conformational steps involved or the coupling between these transitions in the channel complex. As the photoconversion of azobenzene photoswitches is essentially immediate17,18, we used optical generation of a lipid-mediator pulse (optical 'lipid clamp') to kinetically characterize the molecular mechanism of lipid recognition, as well as the cooperativity of DAG-activation, for TRPC3-WT and G652A mutant channels.

We analyzed the kinetics of the initial cycle of fast current activation and deactivation in response to light at a fairly physiological membrane potential of − 40 mV. Taking advantage of the temporal precision of the optical 'lipid clamp' approach, we collected kinetic information on the molecular processes of TRPC channel activation and deactivation. As shown in Figure 6a, activation (on) kinetics were sigmoidal in nature, suggesting that the active lipid mediator triggered channel opening by a process that requires multiple conformational transitions. Sigmoidal activation kinetics were observed with both OptoDArG and PhoDAG-1 (Supplementary Figure 9). Inspection of the delayed, sigmoidal onset of current activation (on-kinetics) during an optical 'lipid clamp' pulse revealed that the WT and G652A channels exhibited substantial differences in their activation kinetics at equivalent stimulation (light) intensities. Quantification of the activation delay by determining the intercepts of single exponential fits relative to the onset of the pulse showed that the mutant channel displayed a significantly reduced activation delay (Figure 6b,d), indicating decreased cooperativity. More direct characterization of sigmoidicity by fitting the current time courses to power exponential functions demonstrated that sigmoidicity was highest for WT currents with a mean power (n) of 5 at maximum light intensity (Figure 6c). G652A currents activated significantly faster with a mean n of 2.9 at maximum light intensities and with a moderately but significantly increased mean n of 4.2 at 50% light intensity. The overall time constants of both current activation and inactivation were not significantly different, and yielded slightly reduced ratios of Toff/Ton for G652A as compared to WT channels (Supplementary Figure 10). Hence, shortening of activation delay by the G652A mutation was associated with reduced sigmoidicity, suggesting either a reduced number of conformational changes or altered relative rate constants of these transitions and therefore a cooperative gating process22.

Our results obtained from optical 'lipid clamp' experiments demonstrate that the G652A mutation has an impact on photoactivation kinetics and suggest that TRPC3 channels are cooperatively activated by lipid mediators via a process involving the critical G652 residue and hence a domain near the selectivity filter.

Discussion

For the first time, we report here on the successful utilization of photopharmacology to gain insights into the sensing and gating processes of a lipid-regulated ion channel. We introduce a newly designed photoswitchable DAG (OptoDArG) that is suitable for efficient control of TRPC conductances with light. Homology modeling combined with an optical 'lipid clamp' approach provided evidence for the existence of a fenestrated subunit interface near the

TRPC3 selectivity filter, which harbors a glycine residue, G652, critical for molecular recognition of lipid mediators by the channel. Our initial biophysical characterization at the single-channel level revealed that lipid-dependent gating was modified in the G652A mutation, whereas the open pore properties remained unchanged. This finding supported the view that G652 played a key role in gating flexibility within the pore domain and encouraged us to test the contribution of pore-domain residues to lipid sensing. Our results obtained at the single-channel level indicated that the G652A mutation reduced sensitivity to lipid-mediated destabilization of closed states in a physiological setting (i.e., when DAGs are generated by cellular PLC activity). To our knowledge, this is the first demonstration of the single-channel gating process that underlies the lipid-mediated activation of TRPC3. The results obtained from classical pharmacological experiments indicated that mutation of G652 affected the channel's ability to discriminate between DAG structures. Interestingly, the G652A mutation showed reduced sensitivity to both PLC activation and SAG, a DAG species that is highly abundant in mammalian phosphoinositides and is considered as a prominent mediator of PLC signaling23,24. To extend our characterization and to determine specific parameters that would provide more direct information on the impact of the mutation on the channel´s lipid sensing machinery, we took a newly developed DAG photopharmacological approach. This strategy enabled us to manipulate lipid mediator levels in the membrane by light17,18 with high temporal precision. In rapid, optical cycling experiments OptoDArG clearly outperformed the recently introduced PhoDAG-1 in its efficiency to control of TRPC3 conductances. The delay and sigmoidicity of the light-induced activation suggested that channel opening requires multiple conformational changes within the channel complex. The simplest activation scheme in this respect involves identical and independent conformational transitions. For a tetrameric complex like TRPC3, an n of 4 is anticipated for single, independent transitions in each subunit. Assuming stable tetrameric assembly, the altered sigmoidicity observed with the G652A mutation indicates a change in the relative rate constants of the transitions, representing a form of cooperativity. We cannot exclude the option that faster association of the lipid with (one or more) recognitions sites contributes to the shorter delay in mutant currents. A higher lipid sensitivity of the mutant along with a certain level of basal DAG in the membrane may produce a shift of conformational states toward channel opening, thereby reducing the activation delay. Nonetheless, our data indicate that multiple lipid recognition domains exist within the multimeric pore complex. This concept of primary recognition of lipophilic channel agonists is reminiscent of the recently described activation of TRPV1 resulting from hydrophobic interactions with residues near its selectivity filter16. A related gating principle has recently been uncovered for the cellular regulation and pharmacology of two pore K^+ channels (K2P)[25,26], which also feature lateral fenestrations within their pore structure. Architecture and flexibility of the TRPC3 pore domain fenestrations may determine lipid recognition, as suggested by altered discriminative features in G652 mutations. Of note, this residue is conserved throughout the TRPC subfamily, and the concept of a general lipid-sensing principle in all TRPC proteins has recently been supported by demonstration of a previously unrecognized DAG sensitivity for TRPC4 and TRPC5 (ref. [27]). Facilitated OptoDArG activation of the TRPC3 G652A mutant, as evident from the lower intensity threshold, a shorter delay and a promotion of increases in residual currents during deactivation, suggests that cooperativity as well as primary lipid recognition features of the channel complex are

indeed affected by this mutation. Thus, we identified G652 as a pivotal element in determining the structure, which plays a key role in the detection of lipid mediators in the channel's vicinity. Whether G652 is itself part of the channel´s primary lipid sensors or an indirect allosteric determinant of its sensing architecture remains to be clarified.

In summary, our photopharmacological characterization of the G652A mutation provided three lines of evidence for the dual role of this amino acid residue in terms of gating rearrangements and recognition of the channel regulator diacylglycerol: G652A displayed (i) a changed pattern of DAG recognition, (ii) altered threshold for lipid regulation and (iii) altered delay and cooperativity of channel activation. By using of a newly designed DAG photoswitch and an optical 'lipid clamp' approach, we gathered evidence for a lipid recognition element that is localized behind the selectivity filter and exposes a series of residues in a subunit-joining region toward the lipid bilayer. Our results lead us to conclude that lipid signaling by TRPC3 involves a 'lipid gating fenestration' located within the pore domain of the channel.

Methods

Methods, including statements of data availability and any associated accession codes and references, are available at https://doi.org/10.1038/s41589-018-0015-6.

Supplementary Material

Refer to Web version on PubMed Central for supplementary material.

Acknowledgements

M. Lichtenegger was a fellow of the BioTechMed Graz program (project: Deciphering the lipid sensing machinery of TRPC channels); O. Tiapko, B. Svobodova and N. Shrestha are members of the PhD program (DK) "Metabolic and Cardovascular Disease" (W1226-B18). The authors wish to thank H. Janovjak for helpful discussions, M. Janschitz for assistance with graphics and T. Schmidt for critically reading the manuscript. The work was supported by FWF (P28701 and P26067 to R. Schindl., P27263 to C.R., P28243 to T.G., W1226-B18 to K.G. and SFB35 subproject F3524 to T.S.) as well as BMWFW HSRSM (PromOpt2.0 to K.G. & C.R.).

References

1. Hofmann T, et al. Direct activation of human TRPC6 and TRPC3 channels by diacylglycerol. Nature. 1999; 397:259–263. [PubMed: 9930701]
2. Bandyopadhyay BC, et al. Apical localization of a functional TRPC3/ TRPC6-Ca2+ -signaling complex in polarized epithelial cells. Role in apical Ca2+ influx. J Biol Chem. 2005; 280:12908–12916. [PubMed: 15623527]
3. Dietrich A, et al. Increased vascular smooth muscle contractility in TRPC6− /− mice. Mol Cell Biol. 2005; 25:6980–6989. [PubMed: 16055711]
4. Neuner SM, et al. TRPC3 channels critically regulate hippocampal excitability and contextual fear memory. Behav Brain Res. 2015; 281:69–77. [PubMed: 25513972]
5. Quick K, et al. TRPC3 and TRPC6 are essential for normal mechanotransduction in subsets of sensory neurons and cochlear hair cells. Open Biol. 2012; 2:120068. [PubMed: 22724068]
6. Poteser M, et al. PKC-dependent coupling of calcium permeation through transient receptor potential canonical 3 (TRPC3) to calcineurin signaling in HL-1 myocytes. Proc Natl Acad Sci USA. 2011; 108:10556–10561. [PubMed: 21653882]

7. Fuchs B, et al. Diacylglycerol regulates acute hypoxic pulmonary vasoconstriction via TRPC6. Respir Res. 2011; 12:20. [PubMed: 21294865]
8. Kim MS, et al. Genetic and pharmacologic inhibition of the Ca2+ influx channel TRPC3 protects secretory epithelia from Ca2+ -dependent toxicity. Gastroenterology. 2011; 140:2107–2115.e4. [PubMed: 21354153]
9. Numaga-Tomita T, et al. TRPC3-GEF-H1 axis mediates pressure overloadinduced cardiac fibrosis. Sci Rep. 2016; 6:39383. [PubMed: 27991560]
10. Phelan KD, Shwe UT, Abramowitz J, Birnbaumer L, Zheng F. Critical role of canonical transient receptor potential channel 7 in initiation of seizures. Proc Natl Acad Sci USA. 2014; 111:11533–11538. [PubMed: 25049394]
11. Smedlund KB, Birnbaumer L, Vazquez G. Increased size and cellularity of advanced atherosclerotic lesions in mice with endothelial overexpression of the human TRPC3 channel. Proc Natl Acad Sci USA. 2015; 112:E2201–E2206. [PubMed: 25870279]
12. Spassova MA, Hewavitharana T, Xu W, Soboloff J, Gill DL. A common mechanism underlies stretch activation and receptor activation of TRPC6 channels. Proc Natl Acad Sci USA. 2006; 103:16586–16591. [PubMed: 17056714]
13. van Rossum DB, et al. TRP_2, a lipid/trafficking domain that mediates diacylglycerol-induced vesicle fusion. J Biol Chem. 2008; 283:34384–34392. [PubMed: 19043047]
14. Zhang L, Saffen D. Muscarinic acetylcholine receptor regulation of TRP6 Ca2+ channel isoforms. Molecular structures and functional characterization. J Biol Chem. 2001; 276:13331–13339. [PubMed: 11278449]
15. Cao E, Liao M, Cheng Y, Julius D. TRPV1 structures in distinct conformations reveal activation mechanisms. Nature. 2013; 504:113–118. [PubMed: 24305161]
16. Gao Y, Cao E, Julius D, Cheng Y. TRPV1 structures in nanodiscs reveal mechanisms of ligand and lipid action. Nature. 2016; 534:347–351. [PubMed: 27281200]
17. Frank JA, et al. Photoswitchable fatty acids enable optical control of TRPV1. Nat Commun. 2015; 6:7118. [PubMed: 25997690]
18. Frank JA, et al. Photoswitchable diacylglycerols enable optical control of protein kinase C. Nat Chem Biol. 2016; 12:755–762. [PubMed: 27454932]
19. Doleschal B, et al. TRPC3 contributes to regulation of cardiac contractility and arrhythmogenesis by dynamic interaction with NCX1. Cardiovasc Res. 2015; 106:163–173. [PubMed: 25631581]
20. Hofmann T, Schaefer M, Schultz G, Gudermann T. Subunit composition of mammalian transient receptor potential channels in living cells. Proc Natl Acad Sci USA. 2002; 99:7461–7466. [PubMed: 12032305]
21. Lichtenegger M, et al. A novel homology model of TRPC3 reveals allosteric coupling between gate and selectivity filter. Cell Calcium. 2013; 54:175–185. [PubMed: 23800762]
22. Zagotta WN, Hoshi T, Dittman J, Aldrich RW. Shaker potassium channel gating. II: transitions in the activation pathway. J Gen Physiol. 1994; 103:279–319. [PubMed: 8189207]
23. Mauco G, Dangelmaier CA, Smith JB. Inositol lipids, phosphatidate and diacylglycerol share stearoylarachidonoylglycerol as a common backbone in thrombin-stimulated human platelets. Biochem J. 1984; 224:933–940. [PubMed: 6525180]
24. Hindenes J-O, et al. Physical properties of the transmembrane signal molecule, sn-1-stearoyl 2-arachidonoylglycerol. Acyl chain segregation and its biochemical implications. J Biol Chem. 2000; 275:6857–6867. [PubMed: 10702245]

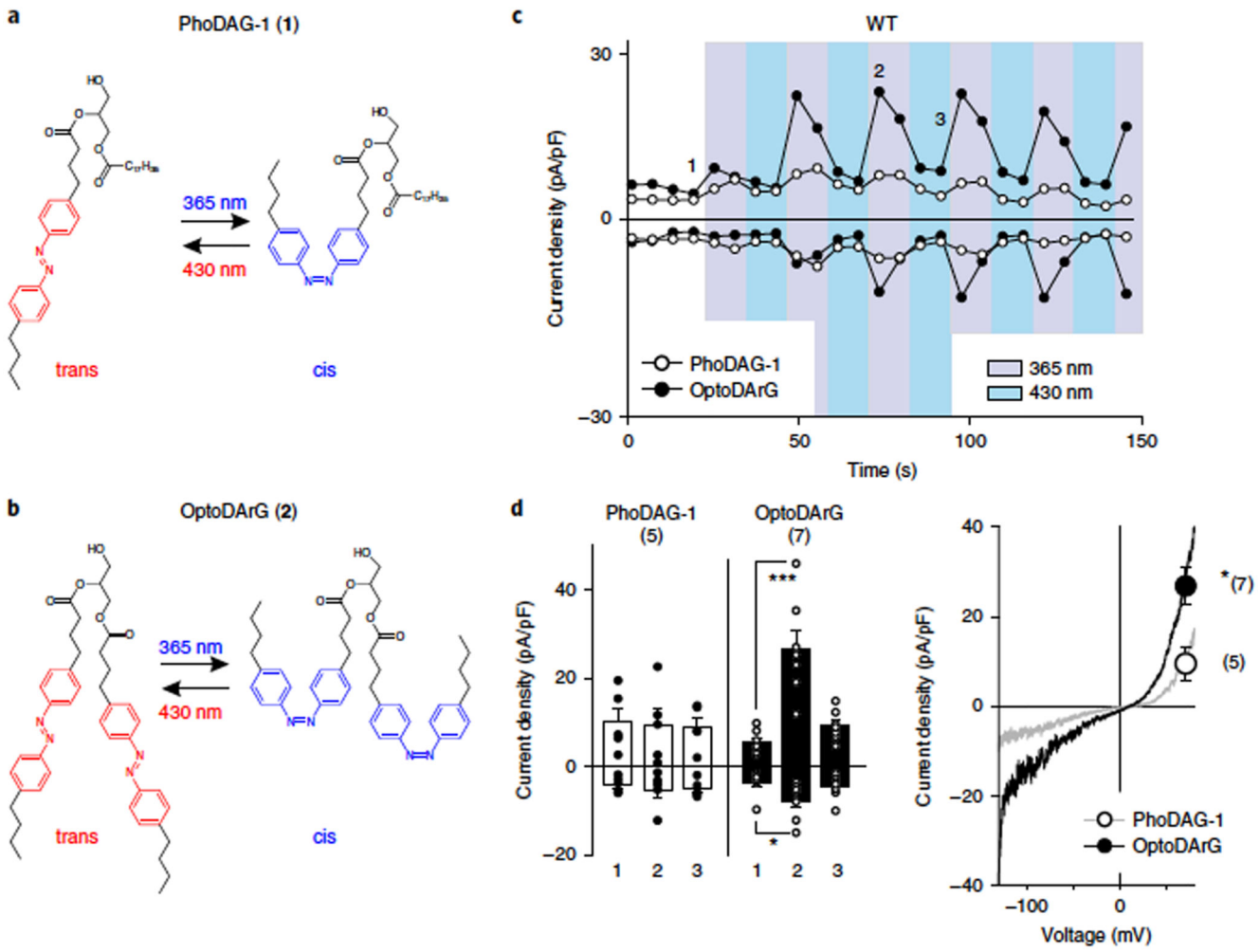

Figure 1. Optical control of TRPC3 conductances expressed in HEK293 cells by DAG photoswitches.

a,b, Chemical structures of photoswitchable DAGs:PhoDAG-1 (ref. 18) (**1**; **a**) and the newly synthesized OptoDArG (2; b; Supplementary Note). c, Representative time courses of the TRPC3-WT conductances recorded at − 90 mV and + 70 mV during repetitive photoconversion of PhoDAG-1 (400 μM, open circles) and OptoDArG (30 μM, closed circles). UV (365 nm; violet) and blue light (430 nm; blue) irradiation are indicated, with each pulse maintained for 10 s. Time points corresponding to mean values given in d for basal (before illumination; 1), activation (2) and deactivation (3) are indicated. **d**, Left panel, current densities induced by photoconversion of PhoDAG-1 (400 μM, white) and OptoDArG (30 μM, black) are shown for TRPC3-WT and G652A (at − 90 mV and + 70 mV; mean ± s.e.m. are shown; N = numbers of cells measured, indicated in parentheses) at time points (1,2,3) given in **c**; two-tailed t-test (normally distributed values) or Mann–Whitney rank sum test (non-normally distributed values) were applied and significant difference at *P < 0.05; ***$P < 0.001$ are indicated; if no P value is given, comparison with basal (1) current levels is not significant. Values from individual experiments are shown for each of the columns (circles). Right panel, representative current to voltage relations of the PhoDAG-1 and

OptoDArG-induced currents as obtained by voltage-ramp protocols measured at blue light irradiation (cis photoconversion) at + 70 mV. Mean current densities ± s.e.m. (N = number of cells measured, indicated in parentheses; corresponding to left panel) for PhoDAG-1 (open circle) and OptoDArG (closed circle); *P = 0.016.

Europe PMC Funders Author Manuscripts

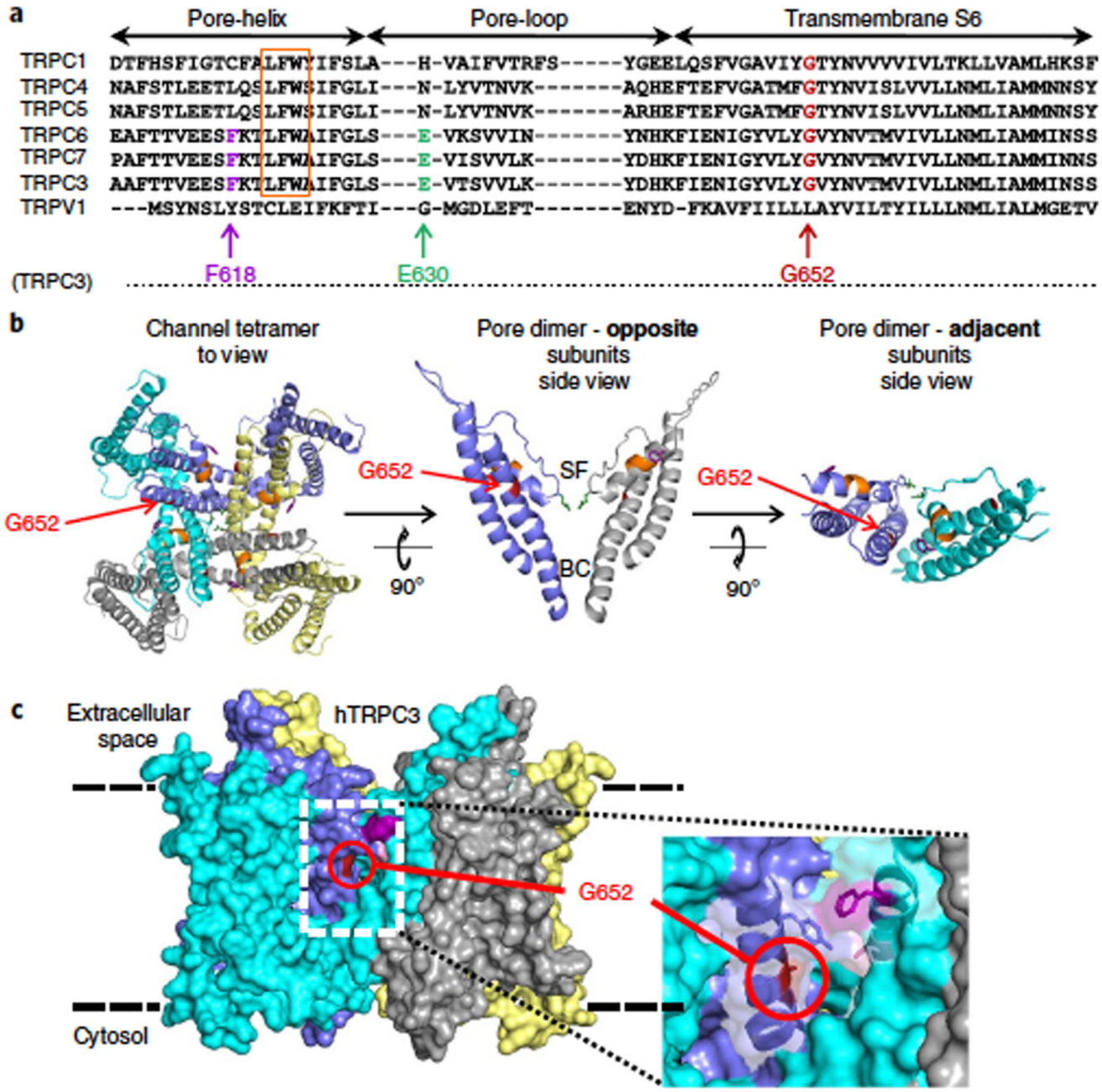

Figure 2. Localization of critical residues within a 'lipid-gating fenestration' in TRPC3. Homology model of human TRPC3 based on the Cryo EM structure of TRPV1 (PDB ID 3J9J).

a) Alignment of conserved residues in regions flanking the TRPC1/3/4/5/6/7 and TRPV1 of pore helix. For TRPC3, G652 (red), F618 (magenta) and E630 (green) are highlighted along with the LFW motif (orange). Residue numbering corresponds to the human TRPC3 (hTRPC3) isoform 3. **b**) Left, top view of four subunits forming the tetrameric TRPC3 channel; G652 is highlighted. Middle, side view of a section showing the poreforming transmembrane helices S5–S6 (residues 570 to 674) of two opposite subunits, with the G652 position indicated relative to the selectivity filter (SF) and the S6 bundle crossing gate (BC).

Europe PMC Funders Author Manuscripts

Right, two adjacent chains displaying the subunit interface with a fenestration exposing G652 to the lipid bilayer from the top. **c**) Space-filling representation of the ‘lipid-gating fenestration’ within the TRPC3 tetramer assembly from an orthoscopic side view.

Europe PMC Funders Author Manuscripts

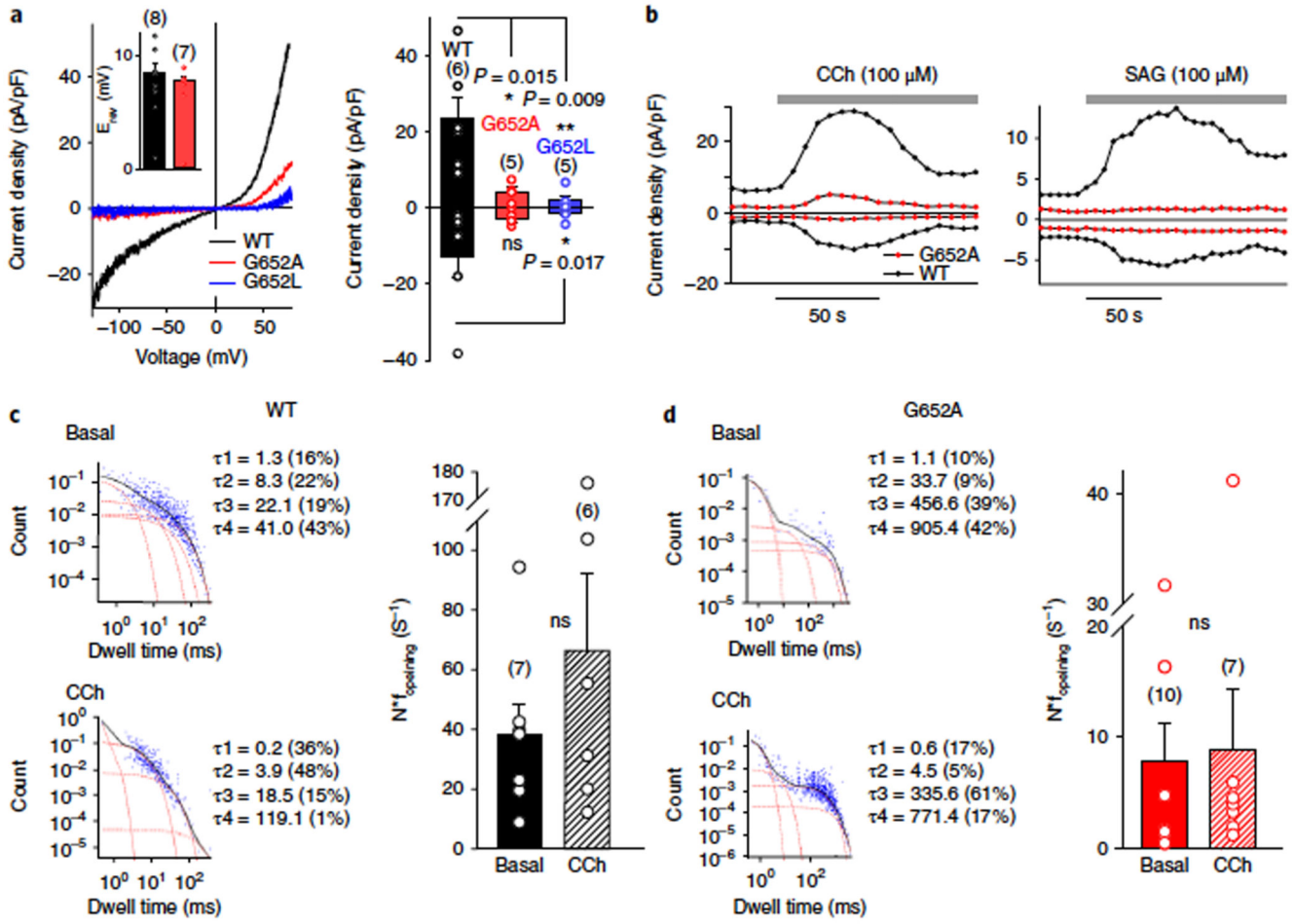

Figure 3. G652 plays a critical role in TRPC3 gating and activation by DAGs.

a) Left, representative I–V relations of carbachol (CCh)-induced currents (100 µM) through TRPC3-WT (black), G652A (red), or G652L (blue) channels expressed in HEK293 cells. The insert shows the mean reversal potential of illustrated currents. Right, histogram displaying mean current densities of CCh-stimulated (100 µM) HEK293 cells, expressing TRPC3-WT (black), G652A (red), or G652L (blue) channels (right). Mean ± s.e.m. are shown; N = number of cells measured, indicated in parentheses; significant difference at **P* < 0.05 and ***P* < 0.01 are indicated. Values from individual experiments are shown for each of the columns (circles). **b)** Representative time courses for current activation by CCh (100 µM, left panel) and SAG (100 µM, right panel) in TRPC3-WT (black) and G652A (red) mutant channels. **c,d**) Closed time distribution of the nonstimulated (basal, upper left panel) and CCh-stimulated (100 µM; lower left panel) TRPC3-WT (c) and G652A channels (d), expressed in HEK293 cells. Data are derived from single-cell-attached patches at a membrane potential of + 80 mV. The sum of four exponential equations (black) and individual components (red line) with time constants (τ_1– τ_4) are indicated (**c,d**, left panel). Right panel of **c,d**, statistics of the characteristic opening frequency (f opening) for TRPC3-WT (**c**) and G652A (**d**) mutant channels under basal- and CCh-stimulated conditions as indicated. Mean ± s.e.m. are shown; *N* = number of cells measured, indicated in parentheses;

Europe PMC Funders Author Manuscripts

two tailed *t*-test (normally distributed values) or Mann-Whitney tests (non-normally distributed values) were applied, ns, not significant ($P > 0.05$). Individual values are shown for each of the data sets (circles).

Europe PMC Funders Author Manuscripts

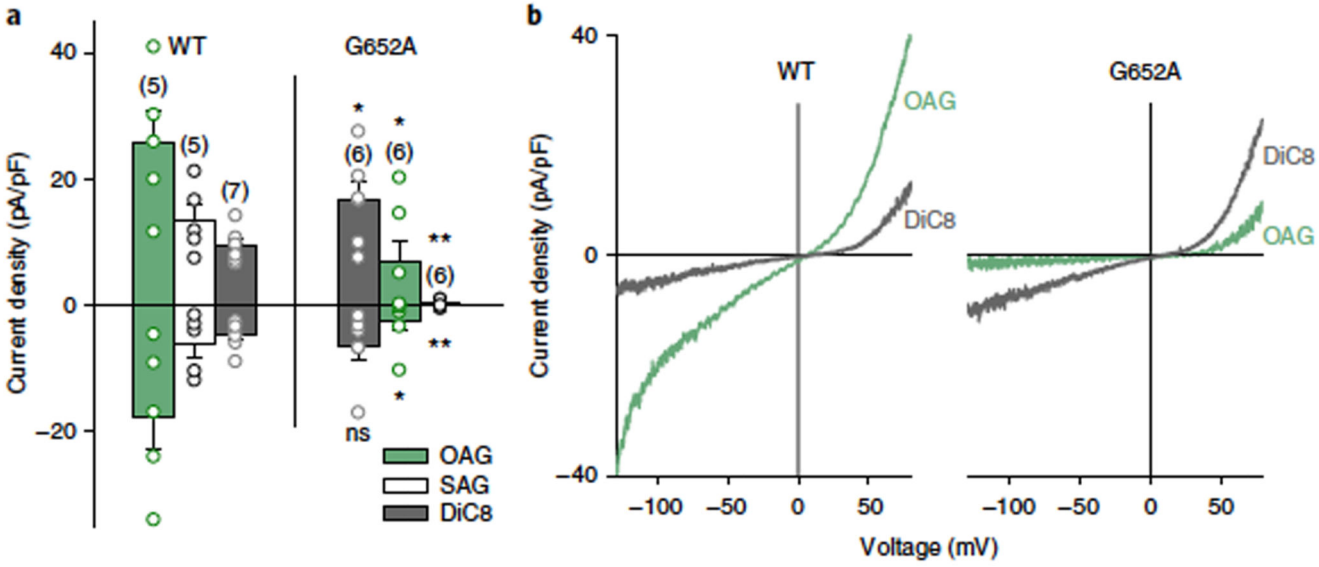

Figure 4. G652A mutation alters discrimination between DAGs by TRPC3.

a)Bar chart illustrating the current density (at − 90 mV and + 70 mV) of the maximal responses obtained in TRPC3-WT and G652A induced by OAG (100 μM; green), SAG (100 μM; white) and DiC8 (100 μM; gray). Data represent mean ± s.e.m.; *N* = number of cells measured, indicated in parentheses; two tailed t-test (normally distributed values) or Mann–Whitney tests (non-normally distributed values) were applied, significant differences at **P* < 0.05; ***P* < 0.01 are indicated; ns, not significant (*P* > 0.05). Values from individual experiments are shown for each of the data sets (circles). **b**) Representative I–V relations recorded in TRPC3-WT and G652A after application of OAG (100 μM; green) and DiC8 (100 μM; gray)

Europe PMC Funders Author Manuscripts

Europe PMC Funders Author Manuscripts

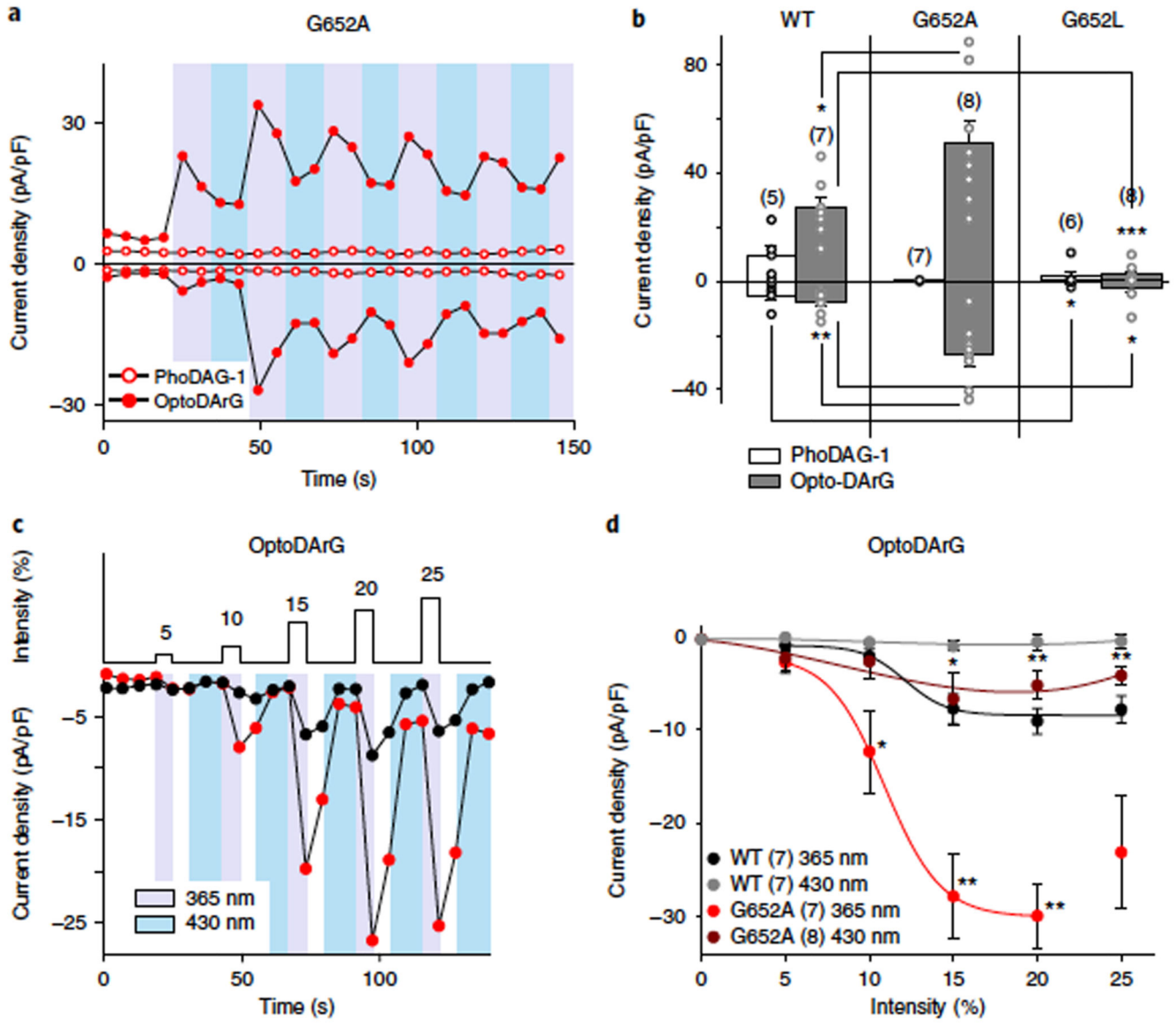

Figure 5. Photopharmacological determination of the DAG sensitivity of TRPC3-WT and G652A channels.

a) Representative time course of the G652A conductance recorded at − 90 mV and + 70 mV during the repetitive photoconversion of PhoDAG-1 (400 μM, open circles) and OptoDArG (30 μM, closed circles). UV (365 nm; violet) and blue light (430 nm; blue) irradiation is indicated, with each pulse maintained for 10 s. Mean values ± s.e.m. are shown for peak; net-current responses are shown in **b**. **b**) Current densities (at − 90 mV and + 70 mV; mean ± s.e.m.; N = number of cells measured, indicated in parentheses) at the maximum, net responses induced by PhoDAG-1 (400 μM, white) and OptoDArG (30 μM, gray) are shown for TRPC3-WT and G652A. Data are mean ± s.e.m.; N = number of cells measured, as indicated; two tailed t-test (non-normally distributed values) or Mann–Whitney test (nonnormally distributed values) were applied and significant differences at $*P < 0.05$; $**P < 0.01$; $***P < 0.001$ are indicated; if no P level is given, comparison with WT (PhoDAG-1)

is not significant ($P > 0.05$). Values from individual experiments are shown for each of the columns (circles). Individual values are shown for each of the columns (circles). **c**) Representative responses to increasing light intensity (maximal output power, 670 mW) of TRPC3-WT-(black) and G652A-(red) expressing HEK293 cells induced by photoisomerization of OptoDArG (30 μM). UV (365 nm, violet, pulse held for 2 s) and blue light (430 nm, blue, pulse held for 10 s) are shown. **d**) Light intensity: current density relation for TRPC3-WT (peak inward current, black; minimum current level during deactivation, gray) and G652A (peak inward current, red; minimum current level during deactivation, deep red) obtained by photoisomerization of OptoDArG (30 μM). Mean ± s.e.m. are shown; N = number of cells measured are indicated; two tailed t-test (non-normally distributed values) or Mann-Whitney tests (non-normally distributed values) were applied; significant difference in comparison to WT indicated at $*P < 0.05$ and $**P < 0.01$.

Europe PMC Funders Author Manuscripts

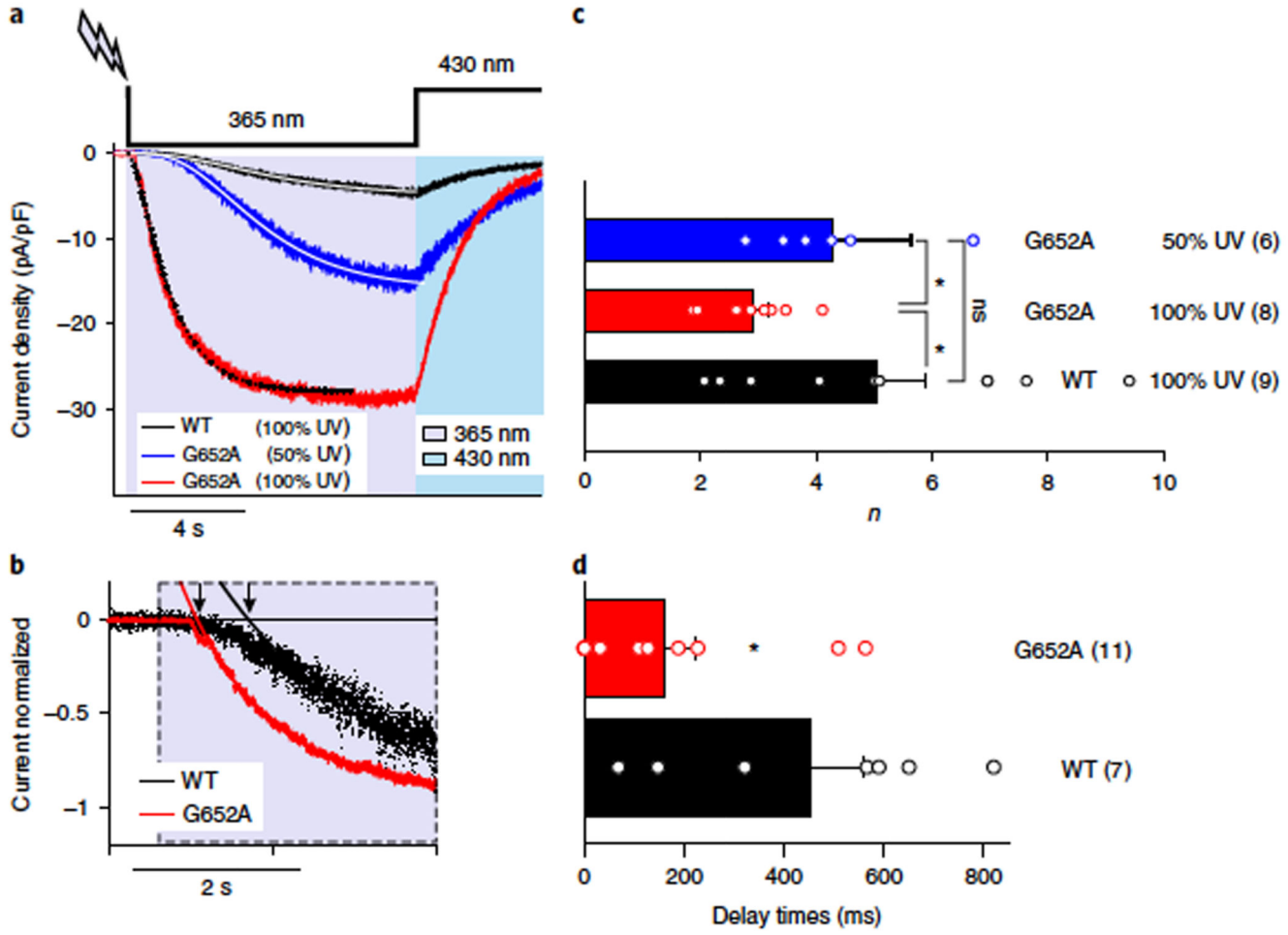

Figure 6. Optical cycling of TRPC3-WT and G652A mutant channels in the presence of OptoDArG (30 μM) occurs with divergent kinetics.

a) Representative traces showing the inward currents induced by OptoDArG (30 μ M) in a whole-cell, gap-free recording (holding potential: − 40 mV, normalized by capacitance) in TRPC3-WT and G652A-expressing HEK293 cells. UV: 365 nm, violet; blue light: 430 nm, blue. TRPC3-WT (black) and G652A (red) responses were induced with 100% intensity of UV, and G652A (blue) was triggered with 50% UV. Exponential fits of current activation for TRPC3-WT (black, 100%), G652A (red, 100%) and G652A (blue, 50%) are shown. **b**) Exponential fits of the initial phase of current activation for TRPC3-WT (black) and G652A (red). Signal was normalized to peak current. The delay of current activation derived from monoexponential fits is indicated by black arrows. **c**) Power (*n*) of power-exponential fitting is shown ($f = A*(1-\exp(-x/tau))^n$). Data are mean ± s.e.m.; *N* = number of cells, indicated in parentheses; two-tailed t-test or Mann-Whitney tests were applied; ns, not significant in comparison to WT. **d**) Histogram displaying the current activation delay for TRPC3-WT (black) and G652A (red). Data are mean ± s.e.m.; *N* = number of cells measured, indicated in parentheses; two-tailed t-test or Mann-Whitney test were applied; $*P < 0.05$. Values from individual experiments are shown for each of the columns (circles).

Europe PMC Funders Author Manuscripts